**Shahid Chamran
University of Ahvaz**

Journal of

Applied and Computational Mechanics

A Hybrid SVM-RVM Algorithm to Mechanical Properties in the Friction Stir Welding Process

Hadi Tagimalek[1], Mohammad Reza Maraki[2], Masoud Mahmoodi[3], Majid Azargoman[4]

[1] Faculty of Mechanical Engineering, Semnan University, Semnan, Iran, Email: h_tagimalek@semnan.ac.ir

[2] Department of Materials and Metallurgy Engineering, Birjand University of Technology, Birjand, Iran, Email: maraki@birjandut.ac.ir

[3] Faculty of Mechanical Engineering, Semnan University, Semnan, Iran, Email: mahmoodi@semnan.ac.ir

[4] Faculty of Mechanical Engineering, Semnan University, Semnan, Iran, Email: m_azargoman@semnan.ac.ir

Abstract. The friction stir welding method is one of the solid-state welding methods for non-homogeneous metals. In this study, the 5XXX series aluminum sample and pure copper are subjected to four passes friction welding process and then the mechanical and metallurgical properties of the welded samples are compared with the prototype. For this purpose, the effect of welding parameters including rotational speed, forward speed and pin angle of the tool is tested by the full factorial method. In this process, hardness estimation and tensile testing are based on input process parameters in order to obtain mechanical properties is an important issue. For this purpose, a mathematical model of mechanical properties must be defined based on the input process parameters. Due to the complex nature of the effect of input process parameters on mechanical properties, this modeling is a complex mathematical problem in which the use of supervised learning algorithms is considered as an efficient alternative. In this paper, a new combination of Relevance Vector Machine (RVM) and Support Vector Machine (SVM) is presented which has a higher degree of accuracy.

Keywords: Friction stir welding, Hardness, Support Vector Machine, Relevance Vector Machine

1. Introduction

Aluminum alloys have been developed in today's industries for use in structural applications, which are mainly classified into two major categories: aluminum cast alloys and used aluminum alloys. Aluminum 5 Series contains 4% magnesium and about 0.25% chromium in the production of fuel and oil pipes, fuel tanks, chemical equipment requiring excellent corrosion resistance, good fatigue strength, weldability, and moderate strength. Freezing defects, the formation of intermetallic compounds, and excessive heat applied to fusion welding processes have made these processes less attractive for bonding to non-homogeneous metals [1]. Bhamji et al. [2] succeeded in bonding aluminum 1050 to copper metal by frictional welding by examining and conducting experimental experiments on aluminum friction welding with copper. Mishra et al. [3] presented a new method of friction welding with a new method for welding aluminum parts in which the heat generated increases as the rotational speed increases and most of the heat generated in this method is supplied by combing of shoulder friction with metal surface. On the other hand, the surface of the shoulder prevents the heated area from contacting the environment with heat and oxidation of the base metal. In a study by Mahoney et al. [4], the friction welding properties of aluminum 7075 show that the high temperature of this region affects the sediment and alloying elements. In a study of the appearance and mechanical properties of the friction welding of copper-aluminum alloys, Liu et al. [5] showed that the different properties of base metal and weld metal can produce oscillatory stresses in

the heat-affected areas and adjacent regions. These stresses cause fatigue in the weld area and eventually lead to crack development and damage to the joint. Ismaili et al [6] conducted experimental studies and experiments with friction welding, aluminum-to-copper sheets as well as aluminum and brass sheets, and found that by studying their mechanical and microstructural properties, they achieved the highest strength comes with 80% strength of the aluminum base metal. They cited the reason for this proper coupling because of the good flow of materials and the creation of narrow multilayer intermetallic compounds in the intermetallic joint. According to the studies carried out in this study, experimental experiments and 5xxx aluminum bonding to copper metal were carried out to obtain desirable results in mechanical properties and numerical modeling and algorithmic design of hybrid enamel with Relevance Vector Machine (RVM) and Support Vector Machine (SVM) that are most capable of predicting test results are discussed.

2. The FSW Process

Despite the suitability of some solid-state bonding processes such as ultrasonic welding, penetration welding and explosive welding for non-homogeneous metal bonding, some limitations of these processes such as geometrical constraints, special equipment requirements, and high cost have led to extensive research on processes Solid-state coupling to remove these limitations [7].

Due to the problems of eliminating the problems caused by the melting heat in the welding pond, the frictional welding method was introduced, where the temperature in the welding zone is about 80% of the melting temperature, which to overcome the problems caused by the melting of aluminum alloys, the friction stir welding process was invented which was a solid-state welding process [8]. Problems arising from fusion welding include:

1. When the metal is melted during welding, the rapid freezing of non-equilibrium structures occurs after bonding. In fact, due to residual stresses, the structure becomes susceptible to cracking. Therefore, heat treatment must be performed on the components to modify the structure. In solid-state welding, no equilibrium structure is formed.

2. When the metal melts, the gas dissolution rate is very high. In melting processes, the surface of the melt is completely exposed to the surrounding environment and gas can be absorbed. These gases lower the solubility in the solid during freezing, and the melt becomes supersaturated. It is very difficult and almost impossible to remove these dissolved gases from the solid bulk. Hydrogen gas causes the worst case because it dissolves in the melt as a proton particle with high mobility. Hydrogen causes cold or late cracking. In solid-state welding, this problem is not due to the absence of melt.

3. During welding, non-uniform extensions and non-uniform contractions occur during freezing, resulting in tensile stresses that are susceptible to cracking; thus, in solid-state welding, the type of stresses remaining in the joint season is the compressive stresses that eliminate the possibility of crack propagation.

The most important parameters of friction stir welding are tool rotation speed, tool speed, and tool angle deviation. In the meantime, the junction tool performs the primary task of warming the workpiece, moving the material to create the junction and also keeping the hot material under the front of the tool. In the research, aluminum metal was bonded to copper metal by the friction welding process of the weld and without flaws. However, most joints in the mechanical tests of the weld line or contact surface of the two metals fail and crack in the weld region. There are some reasons to justify this that the most important of these can be the formation of brittle intermetallic compounds as well as the formation of an oxide layer that has less strength in the vicinity of intermetallic compounds [9 and 10]. Fig. 1 schematically illustrates the frictional stir welding process.
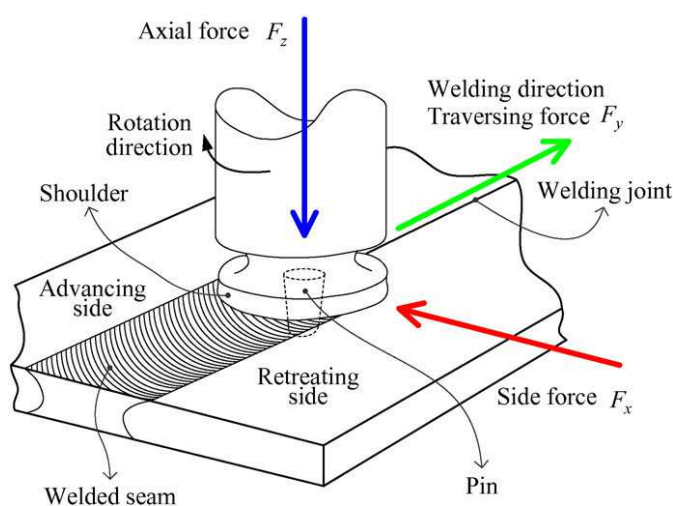

Fig. 1. Schematic of the friction stir welding process [5]

3. Experimental Details

In this study, aluminum and pure copper sheets of 3 mm thickness were used and the mechanical properties of base metals are shown in Table 1. The tools used were two types of cylindrical and square pins of H13 hot steel with a hardness

of 52 Rockwell. The FP4M milling machine manufactured in Tabriz was used to rotation and forward the tools. Tool geometry is the most important factor in the frictional welding process and plays the most important role in material flow. A friction stir welding tool consists of a pin and a shoulder. The function of the tool is to generate local heat and material flow. The first function is to generate heat at the beginning of the pin's contact with the material due to friction. Some heat also comes from the plastic deformation of material. The pin sinks as far as the shoulder sits on the workpiece surface. The friction between the shoulder and the workpiece at this stage produces much of the heat of the process. In terms of heat generation, the ratio of pin and shoulder size is also important. However, other design parameters have little effect on the heat produced. The shoulder also determines the warming range of the piece. The second function of the tool is to rotate and move the material. The formation of the microstructure and the resulting properties depend on the geometry of the tool. A concave shoulder and threaded cylinder pin are commonly used. In the circular tool pin, the material's displacement volume is reduced by up to 60% and in the square tool by up to 70%. The advantage of these designs is the reduction of frictional force, the possibility of moving part of the material that has deformed the plastic, facilitating the collapsing motion of the tool, and increasing the Intersection joint between the pin and the material that deforms the plastic, as more heat is produced. The main advantage of these pins is the dynamic-to-static volume ratio, which is important for creating a proper path for material flow. Given the important geometrical effect of the tool on the metal flow, the resulting microstructure, which is directly related to the flow pattern, will be different for each tool.

Table 1. Mechanical properties of base metals

Mechanical Properties	Cu	Al 5XXX
Tensile Strength (MPa)	392	223
Yield Strength (MPa)	236	329
Hardness (Vickers)	104	108

Fig. 2. FP4M milling machine used in experimental tests
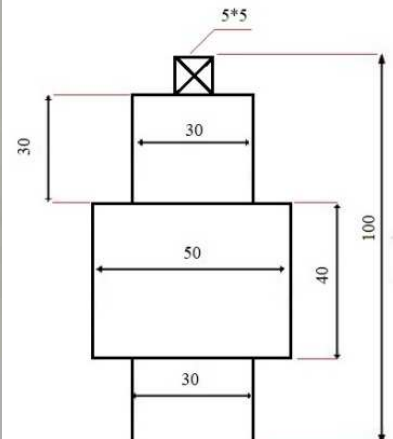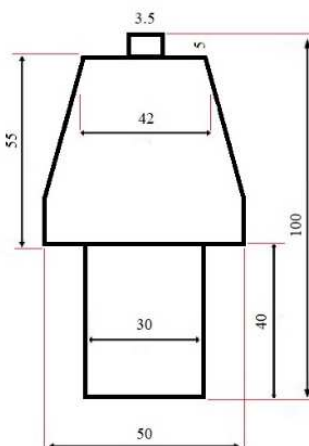

Fig. 3. Hot steel welding cylindrical tool with square and cylindrical pin

In order to carry out the design of experiments and to obtain an acceptable algorithm, it has been attempted to apply step by step the design process of a full factorial experiment. To perform complete tests to achieve proper process control, a large amount of testing must be performed. One of the main goals of test design methods is to select the best possible test mode that can be used to evaluate the process while justifying the number of experiments, in the most desirable way possible the Minitab software is used. In this range, input variables have been studied and the maximum and minimum limits of theory and practical constraints have been determined. Using the full factorial method, 72 experiments are presented in Table 2. The test pieces were prepared according to ASTM E8-04 standard for the tensile test and the test at a constant speed of 1 mm/min and a strain rate of 0.003 at room temperature for all welded specimens by the SANTAM STM-150 in Semnan University.

The hardness of the welded specimen was metallography according to ASTM-E384 by Vickers hardness test with Bohler machine at 250 g force for 10 seconds. Hardness was measured at five points 2 mm apart on the cross-section of the welded specimen.
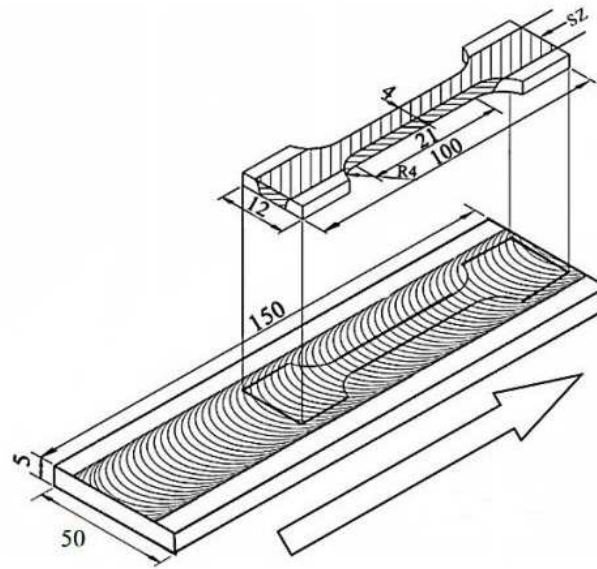

Fig. 4. Schematic of stretch specimens (in millimeters) according to ASTM E8-04
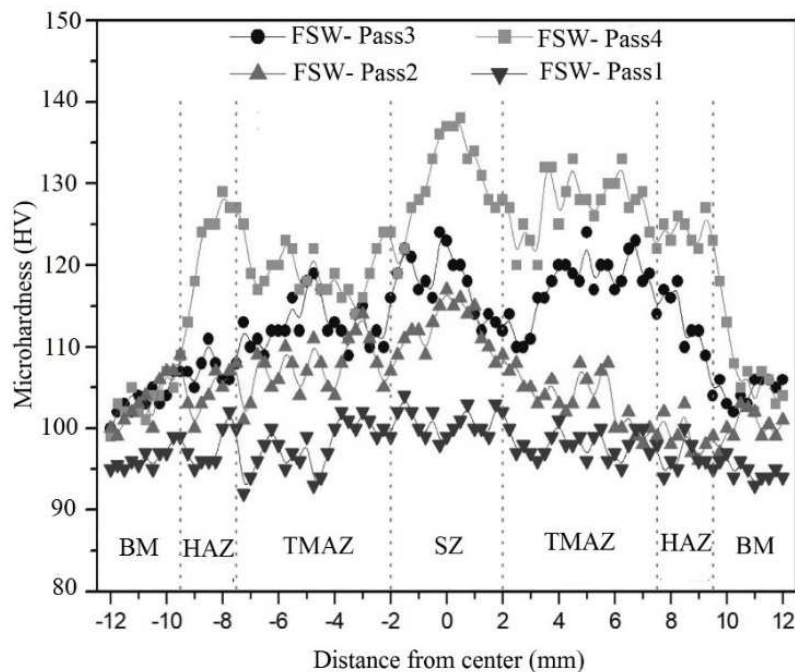

Fig. 5. Micro hardness diagram of welding samples in four different passes

Table 2. Input parameters of friction stir welding process

NO	Welding Parameters	Units	Range
1	Pin angle	Degree	2-3
2	Rotational speed	RPM/min	700-850-1000-1150
3	Forward speed	mm/min	22-40

Table 3. Empirical experiments and model obtained with effective parameters

Exp. No	Pin Geometry	Forward Speed	Rotational Speed	Pin Angle	Hardness	Tensile Strength
1	Cylindrical	40	700	4	95.4	162.8
2	Cylindrical	32	700	3	96.1	164.7
3	Square	27	700	2	98.2	165.1
4	Square	40	850	2	96.01	166.8
5	Square	40	1000	2	98.3	169
6	Cylindrical	40	850	2	99.15	167.2
7	Cylindrical	32	850	4	99.6	163.2
8	Cylindrical	27	1150	4	101.2	167.3
9	Square	40	1000	3	100.5	168.9
10	Cylindrical	27	700	2	104.9	170.5
11	Cylindrical	40	700	3	102.5	169.9
12	Cylindrical	32	1000	4	102.3	179.6
13	Square	32	700	2	99.2	166
14	Square	32	1150	4	99.8	183
15	Square	40	1150	4	100	178.9
16	Cylindrical	27	1000	4	105.3	170.1
17	Square	32	1150	2	107.9	170.2
18	Square	32	850	4	100	190
19	Square	27	1150	4	98	175.3
20	Square	40	850	4	99.6	159
21	Cylindrical	27	850	4	100.9	163
22	Cylindrical	27	1150	2	99.8	188.3
23	Cylindrical	32	850	2	97.5	171.1
24	Square	32	1150	3	100.1	187.3
25	Cylindrical	27	1150	3	120.9	195
26	Cylindrical	40	1000	3	118.9	189.6
27	Cylindrical	32	1150	3	117.3	192
28	Cylindrical	40	1000	4	115	187.6
29	Cylindrical	40	850	3	102.3	186.6
30	Cylindrical	32	850	3	104.3	185
31	Square	27	700	3	101.8	179
32	Cylindrical	32	1150	4	105.6	189.6
33	Square	40	1000	4	107.7	188.3
34	Square	32	1000	2	109.2	190.2
35	Cylindrical	40	1000	2	104.9	191.2
36	Cylindrical	27	700	4	100	177.4
37	Square	27	1000	2	99.6	177.8
38	Cylindrical	27	1000	2	101.3	180.1
39	Cylindrical	40	1150	3	102.5	179.6
40	Square	27	1150	2	108.9	181.9
41	Square	40	700	3	97.8	185.6
42	Square	32	850	2	99.2	191.5
43	Square	32	1000	4	100	190
44	Cylindrical	40	700	2	95.6	188.2
45	Cylindrical	27	850	3	98.8	190.1
46	Square	27	700	4	97.2	189.5
47	Cylindrical	27	700	3	99.2	190.2
48	Square	32	700	3	97	187.3
49	Square	27	850	4	99.1	188.3
50	Square	27	850	3	95.9	185.3
51	Square	27	1000	4	97.9	187
52	Cylindrical	32	700	4	97.8	185.7
53	Square	32	700	4	94.5	187.6
54	Cylindrical	40	850	4	96.6	188.9
55	Square	27	1000	3	97.2	189.6
56	Square	40	1150	2	99.8	191.1
57	Square	27	1150	3	100	190
58	Cylindrical	40	1150	2	110.8	202.5
59	Cylindrical	32	1150	2	110	201.8
60	Square	27	850	2	98	197.4
61	Square	40	1150	3	97.1	190.3
62	Square	32	850	3	95.8	189.9
63	Cylindrical	27	850	2	106.8	170.1
64	Cylindrical	40	1150	4	114.2	187.6
65	Cylindrical	27	1000	3	116.1	187.3
66	Cylindrical	32	1000	3	113.9	188
67	Square	40	700	4	97.2	97.8
68	Cylindrical	32	700	2	98.6	100
69	Square	40	700	2	100	98.8
70	Square	32	1000	3	100.3	99.9
71	Square	40	850	3	99.9	100.9
72	Cylindrical	32	1000	2	113.5	107.9

According to the results of the tests, the hardness of the leading part was greater than that of the back part, and the reason for this hardness was the same in the direction of rotation and speed of the tool, but in the opposite direction, they acted in the opposite direction. As a result, the heat generated by the leading side increases and the material trapped by the instrument undergoes severe deformation in the perturbation region, which increases the dynamic recrystallization drive force. With the increase of the driving force, there are more reforms on the leading side than on the backside, and the leading part hardness increases.

4. Models

4.1 Supporter Vector Machine

In recent decades, rapid advances in information processing systems have triggered the need for systems that can learn from limited information and solve complex decision problems. The study and construction of algorithms that are able to learn from and make predictions based on a limited set of observed data are explored in a subfield of computer science known as machine learning. In supervised learning, given a set of N input vectors X_n and the corresponding targets t_n, the goal is to learn a model of the dependency of the targets on the inputs in order to predict the targets in case of unobserved inputs [11].

Support vector machines (SVMs) are supervised learning models with associated learning algorithms that analyse data and recognize patterns, used for classification and regression analysis. Structural risk minimization alongside with minimization of empirical risk is the main advantage of the SVMs over the neural networks resulting in a better generalization capability in many practical applications [12, 13].

In SVM-based regression, in order to estimate a function in the form of equation (1) based on a limited set of observations, the input space is mapped into a high dimensional feature space via the kernel function $\Phi(x)$ and then linear optimal regression is performed in this space.

$$y = f(x) = w^T \phi(x) + w_0 \tag{1}$$

The vector of weights W and the bias W_0 are estimated based on structural risk minimization principles [14], by solving the following optimization problem:

$$\min \left\{ R(w) = \frac{1}{2} w^2 + C. \sum_{i=1}^{N} \xi_i + \xi_i^* \right\} \tag{2}$$

where C is the regularization factor, ε is the insensitivity parameter and ε_i and ε_i^* are slack variables, calculated based on the Vapnik's ε-insensitive loss function, as:

$$\xi = \left| y - f(x) \right|_\varepsilon = \max \left\{ 0. \left| y - f(x) \right| - \varepsilon \right\} \tag{3}$$

Fig. 6 illustrates the concept of ε-insensitivity in SVM-based regression. The optimization problem can be solved via quadratic programming optimization and the estimated function is expressed based on the optimal values as:

$$f(x) = y(x_i, w) = \sum_{i=1}^{N} w_i K(x.x_i) + w_0 \tag{4}$$

where N is the number of training samples and K(x, x_i) is calculated as:

$$K(x_k.x_i) = \varphi(x_k).\varphi(x_i) \quad , \quad (k. i = 1 ..... N) \tag{5}$$

The training samples associated with non-zero weights called the support vectors, determine the number of necessary kernel functions for estimating a function. The Gaussian radial basis function (RBF) kernel is the most popular kernel function in SVM and other kernel methods, expressed as:

$$K(x.x_i) = \exp \left(-\frac{x - x_i^2}{2\sigma^2} \right) \tag{6}$$

SVM makes non-probabilistic point predictions. Ideally, estimation of a conditional distribution of the outputs P(t|x) is desired in order to capture the uncertainty in prediction. Although posterior probability estimates have been coerced from SVMs via post-processing, they have been argued to be unreliable [15].

Although relatively sparse, SVMs make liberal use of kernel functions, the requisite number of which grows steeply with the size of the training set. The necessity to estimate the regularization parameter C causes a trade-off between the error, margin, and the insensitivity parameter ε, as the margin of tolerance in function estimation. Therefore, a cross-validation procedure is mainly required, which wastes both data and computation. The kernel function K (x, x_i) must satisfy the mercer's condition. To this end, it must be the continuous symmetric kernel of a positive integral operator.
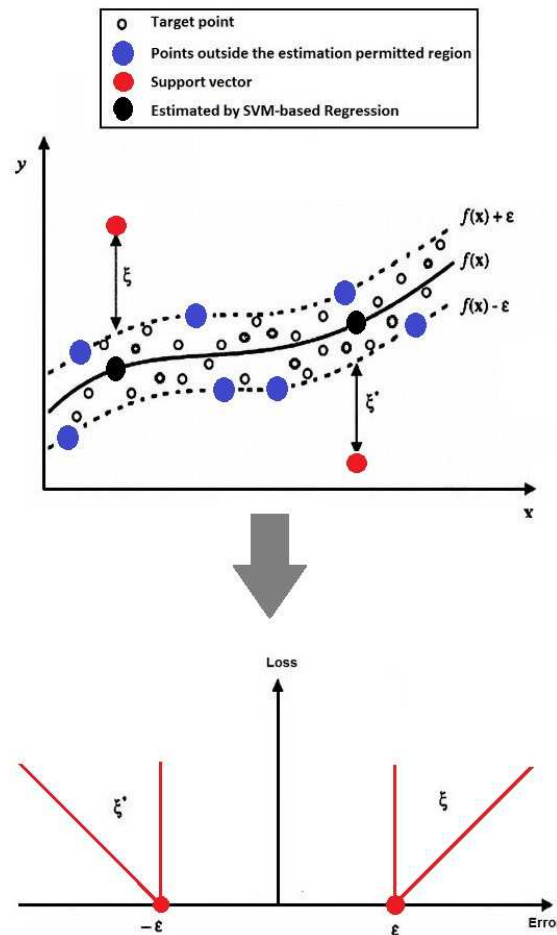
Fig. 6. The ε -insensitivity in SVM-based regression

4.2 Relevance Vector Machine

To overcome the shortcomings of support vector machines, Tipping has proposed a fully probabilistic framework termed relevance vector machine (RVM) [16]. RVM is a nonlinear pattern recognition model with a simple structure based on Bayesian Theory and Marginal Likelihood. In addition to improving the inadequacies of SVM, RVM makes use of a very fewer number of kernel functions. Therefore, it has been used in a broad range of applications from wind power grouping forecast to pneumatic actuator fault diagnosis [17, 18]. However, its application has not yet been investigated for modeling the FSW process. In RVM-based regression, in order to predict a function based on a set of N input-target pairs$\{X_n, t_n\}$, each target is modeled as a function of the corresponding inputs with additive white Gaussian noise to accommodate measurement error on the target:

$$t_i = y(x_i.w) + \varepsilon_i \tag{7}$$

where ε_i is assumed to be mean-zero Gaussian with variance σ^2 and similar to the SVM, y (x, w) is considered as a linear combination of N kernel functions centered at the training samples inputs, in form of equation (1). Therefore, with the assumption that we know y (x_n), each target is independently distributed as Gaussian with the mean y (x_n) and variance σ^2, expressed as:

$$p(t_n|x) = N(t_n|y(x_n).\sigma^2) \tag{8}$$

Based on the assumption of independence of the targets, the likelihood function of the whole samples can be written as:

$$p(t|w.\sigma^2) = \frac{e^{\left\{\frac{-t-\varphi\ w^2}{2\pi\sigma^2}\right\}}}{\left(2\pi\sigma^2\right)^{\frac{N}{2}}} \tag{9}$$

where

$$t = \left(t_1 \dots t_N\right)^T \tag{10}$$

$$w = \left(w_0 \ldots w_N \right)^T \tag{11}$$

and ϕ is an N*(N+1) matrix, defined as:

$$\varphi = \left[\varphi(x_1), \varphi(x_2), \ldots, \varphi(x_N) \right]^T \tag{12}$$

In which the vector $\phi(x_n)$ is calculated as:

$$\varphi(x_n) = \left[1. K(x_n. x_1). K(x_n. x_2)..... K(x_n. x_N) \right]^T \quad , N = 1, \ldots, N \tag{13}$$

It is expected that the maximum likelihood estimation of W and σ^2 from (9) would lead to over-fitting [15]. Therefore, additional constraints must be imposed on the parameters. For this purpose, a prior zero-mean Gaussian probability distribution is assumed for the weights as follows:

$$p(w|\alpha) = \prod_{i=0}^{N} N(w_i | 0. \alpha_i^{-1}) \tag{14}$$

where α is a vector of N+1 hyper-parameters. The variance of this Gaussian probability distribution, α_i^{-1} controls the deviation of each weight from zero, and a very large value for α_i means that the corresponding weight, W_i is estimated to be zero. Using Bayesian posterior inference, the posterior over w is computed as [19]:

$$p(w|t. \alpha. \sigma^2) = \frac{p(t|w. \sigma^2) \; p(w|\alpha)}{p(t|\alpha. \sigma^2)} = (2\pi)^{-\frac{N}{2}} \; |\Sigma|^{-\frac{1}{2}} \; e^{\left\{ -\frac{(w-\mu)^T \Sigma^{-1} (w-\mu)}{2} \right\}} \tag{15}$$

where $\sum$ and μ are calculated as:

$$\Sigma = \left(\sigma^{-2} \varphi^T \varphi + A \right)^{-1} \tag{16}$$

$$\mu = \sigma^{-2} \sum \varphi^T \, t \tag{17}$$

where in A is a diagonal matrix formulated as:

$$A = \text{diag}(\alpha_0, \alpha_1, \ldots, \alpha_N) \tag{18}$$

Integrating P (w|t, α, σ^2) over the weights w, it can be concluded that

$$p(t|\alpha. \sigma^2) = \int p(t|w. \sigma^2) \, p(w|\alpha) \, d \, w \tag{19}$$

The integral above, which is a convolution of Gaussians can be obtained as:

$$p(t|\alpha. \sigma^2) = (2\pi)^{-\frac{N}{2}} \; |\Omega|^{-\frac{1}{2}} \; e^{\left\{ -\frac{t^T \Omega^{-1} t}{2} \right\}} \tag{20}$$

In the above equation, Ω is a matrix defined as:

$$\Omega = \sigma^2 \, I + \varphi \, A^{-1} \varphi^T \tag{21}$$

Learning process of RVM can be described as a search for the parameters α and σ^2 which maximize the marginal likelihood p (t|α, σ^2) based on the training dataset. The optimal parameters cannot be obtained in closed form, and they are estimated using an iterative re-estimation procedure. Based on the approach of MacKay [20], the following iterative relationship can be achieved for estimation of the hyper-parameters α_i by differentiating p (t|α, σ^2) in equation (20) with respect to log (α_i) and equating it to zero.

$$\alpha_i^{new} = \frac{1 - \alpha_i \sum_{ii}}{\mu_i^2} \tag{22}$$

where μ_i is the i-th element of the vector μ in equation (17), and the i-th diagonal element of the matrix $\sum$ in equation (16). For the noise variance σ^2, the following update formula is obtained by setting the derivative of the marginal likelihood with respect to log (α_i) to zero:

$$\left(\sigma^2 \right)^{new} = \frac{t - \varphi\mu^2}{N - \sum_{i=0}^{N} \left(1 - \alpha_i \sum_{ii} \right)} \tag{23}$$

The parameters α_i and σ^2 from equation (22), equation (23) are calculated iteratively, while simultaneously the posterior statistics $\sum$ and μ from equation (16), equation (17) are updated. This procedure is repeated until some suitable convergence criteria have been satisfied. In this procedure, many of the hyper-parameters α_i tend to infinity, which means that the probability distribution of the corresponding weights, W_i is peaked at zero and they are estimated to be zero, thus pruning many of the kernel functions used in equation (1), which leaves the model sparse. The training set, which associates with the remaining nonzero weights is called the relevance vector.

After convergence of the hyper-parameter estimation procedure and obtaining the maximizing values α_{MP} and σ^2_{MP}, the predictions are made based on the posterior distribution over the weights conditioned on them. The predictive distribution for a new input sample x^* is proved by [15] to have a Gaussian distribution, expressed as:

$$p(t^* | t) = N(t^* | y^* . \sigma^2_*) \tag{24}$$

where y^* and σ^2 are the predicted mean and variance values, calculated as:

$$y^* = \mu^T \varphi(x^*) \tag{25}$$

$$\sigma^2_* = \sigma^2_{MP} + \varphi(x^*)^T \sum \varphi(x^*) \tag{26}$$

$$\varphi(x^*) = \left[1. K(x^*. x_1), K(x^*. x_2), ..., K(x^*. x_N)\right]^T , N = 1, ..., N \tag{27}$$

4.3 Results

From the database of weld mechanical properties shown in Table 1, 62 samples (about 86%) were used to train the models and the models' accuracy was evaluated based on the rest ten samples (about 14%), which are marked in bold. Before training and testing the models, all the input and output values were normalized between −1 and +1 based on Eq. (28).

$$un = \frac{2*u - (MX + MN)}{(MX - MN)} \tag{28}$$

In this equation, μ is the input or output, μn is the corresponding normalized value and the maximum or minimum value of the input and output among the whole dataset is indicated by MX and MN respectively.

In progress, the svm-km toolbox [21] and the *Sparse Bayes* package for Matlab [30] used to train the SVM and RVM models, respectively. Based on trained models and the training and test input samples, the predicted training and test outputs were obtained and were scaled to their original range based on Eq. (29).

$$\hat{y} = y_n * \left(\frac{MX - MN}{2}\right) + \left(\frac{MX + MN}{2}\right) \tag{29}$$

wherein, the normalized and final predicted values of the output are denoted by y_n and $\hat{y}$ respectively.

Finally, the root means square error (RMSE) and the coefficient of determination R^2 statistical indices, defined as Eq. (30) and Eq. (31) were calculated to evaluate the models' precision.

$$RMSE = \sqrt{\frac{\sum_{i=1}^{N} (t_i - y_i)^2}{N}} \tag{30}$$

$$R^2 = 1 - \frac{\sum_{i=1}^{N} (t_i - y_i)^2}{\sum_{i=1}^{N} (t_i - M)^2} \tag{31}$$

In these equations, N is the number of samples, t_i and y_i are the targets and the predicted outputs, respectively, and M is the mean value of the targets, calculated as:

$$M = \frac{\sum_{i=1}^{N} t_i}{N} \tag{32}$$

The calculated value of indices is listed in Table 2. For the purpose of comparison, the ratio of RMSE to maximum value of the measured outputs y_{max} is also added to the table. The RVM and SVM kernel and model parameters are also listed in Table 3. As can be observed, in case of the bead width, the RVM method benefits from higher testing accuracy, while in the case of the bead height the SVM method is more accurate. Therefore, a hybrid combination of the two approaches was selected by averaging the two outputs, which benefits from reasonable accuracy for both of the outputs.

Table 4. Statistical indices for evaluation of the RVM and SVM models

Output	Method	RMSE	RMSE/y_{max}	R^2
	RVM	0.0962	0.0301	0.9832
Tensile Test	SVM	0.1094	0.0352	0.9701
	Hybrid RVM-SVM	0.089	0.0307	0.9584
	SVM	0.4577	0.061	0.7939
Hardness	RVM	0.4936	0.0369	0.8369
	Hybrid RVM-SVM	0.5021	0.0412	0.8979

Table 5. The RVM and SVM parameters

Output	Parameter	R^2
	RVM kernel parameter	6.18
Bead Width	SVM kernel parameter	12.008
	SVM regularization factor (C)	10000
	SVM insensitivity parameter (ε)	5-10
	RVM kernel parameter	5.97
Bead Height	SVM kernel parameter	2
	SVM regularization factor (C)	1
	SVM insensitivity parameter (ε)	5-10
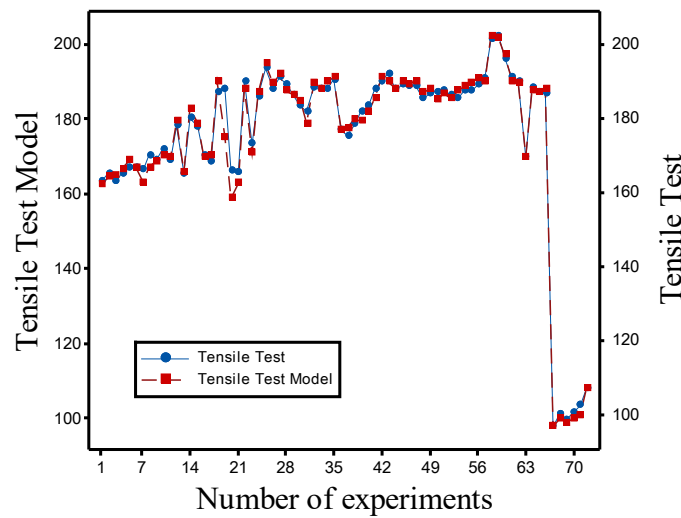
Fig. 7. The predicted values of bead width and the corresponding targets
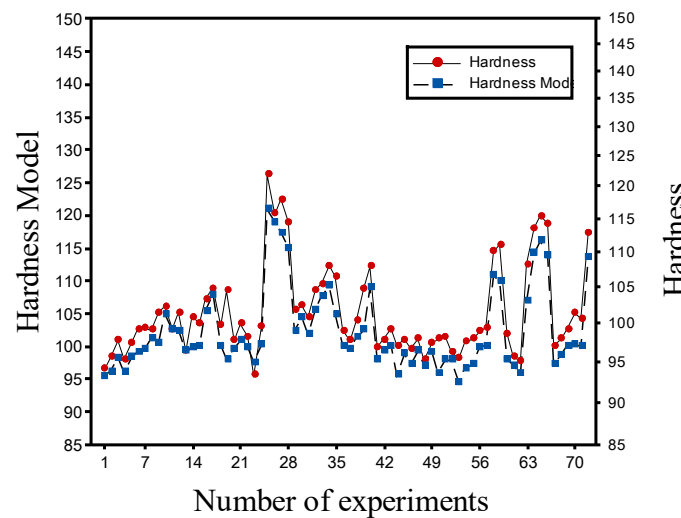
Fig. 8. The predicted values of bead width and the corresponding targets

5. Conclusion

FSW process is a very efficient method for welding non-homogeneous metals. In this process, in order to build high-quality products, it is very important to predict the mechanical properties based on the input welding process parameters. In this paper, a novel hybrid model based on the relevance vector machine and support vector machine regression analysis for modeling and prediction of the weld mechanical properties in the Stir friction welding process was proposed. The input

parameters were considered of Pin geometry, Rotational speed, Pin angle, and Forward speed. The RVM and SVM kernel and model parameters were calculated and a hybrid combination of the two approaches was selected by averaging the two outputs. The coefficient of determination (R^2) was obtained as 0.9584 and 0.8979 for the Tensile Test and Hardness respectively in the case of the test dataset, which indicates the model accuracy for both of the outputs. Based on the hybrid SVM-RVM models, the input parameters can be tuned to obtain desired mechanical properties in this welding process precisely.

Author Contributions

Tagimalek and Maraki planned the scheme, initiated the project and suggested the experiments; Tagimalek and Mahmoodi conducted the experiments and analyzed the empirical results; Azargoman and Tagimalek developed the mathematical modeling and examined the theory validation. The manuscript was written through the contribution of all authors. All authors discussed the results, reviewed and approved the final version of the manuscript.

Acknowledgments

Conflict of Interest

The authors declared no potential conflicts of interest with respect to the research, authorship, and publication of this article.

Funding

Data Availability Statements

The datasets generated and/or analyzed during the current study are available from the corresponding author on reasonable request.

Nomenclature

W, W_0	Weight vector	σ^2	Variance
ε_i	Slack variables	y^*	Predicted mean
C	Regularization factor		

References

[1] Le, V.S., Ghiotti, A., Lucchetta, G., Preliminary studies on single point incremental forming for thermoplastic materials, *International Journal of Material Forming*, 1, 2008, 1179-1182.

[2] Bhamji, I., Moat, R.J., Preuss, M., Thread gill, P.L., Addison, A.C., Peel, M.J., Linear friction welding of aluminum to copper, *Journal Science and Technology of Welding and Joining*, 17, 2012, 314-320.

[3] Mishra, R.S., Ma, Z.Y., Friction stir welding and processing, *Materials Science and Engineering: R: Reports*, 50(1-2), 2005, 1-78.

[4] Ham, M., Jeswiet, J., Single point incremental forming and the forming criteria for AA3003, *CIRP Annals Manufacturing Technology*, 55, 2006, 241–244.

[5] Liu, Z., Li, Y., Meehan, P.A., Experimental investigation of mechanical properties formability and force measurement for AA7075-O aluminum alloy sheets formed by incremental forming, *International Journal of Precision Engineering and Manufacturing*, 14, 2013, 1891–1899.

[6] Esmaeili, A., Rajani, H.R.Z., Sharbati, M., Besharati Givi, M.K., Shamanian, M., The role of rotation speed on intermetallic compounds formation and mechanical behavior of friction stir welded brass/aluminum 1050 couple, *Intermetallics*, 19, 2011, 1711-1719.

[7] Mahoney, M.W., Rhodes, C.G., Flint off, J.G., Bingel, W.H., Spurling, R.A., Properties of friction stir welded 7075 T651 aluminum, *Metallurgical, and Materials Transactions A*, 29, 1998, 1955-1964.

[8] Echrif, S.B.M., Hrairi, M., Research and progress in incremental sheet forming processes, *Materials and Manufacturing Processes*, 26, 2011, 1404-1414.

[9] Jeswiet, J., Micari, F., Hirt, G., Bramley, A., Duflou, J., All wood, J., Asymmetric single point incremental forming of sheet metal, *CIRP Annals Manufacturing Technology*, 54, 2005, 88-114.

[10] Mehrabi, M., Sharifpur, M., Meyer, J.P., Viscosity of Nanofluids based on an artificial intelligence model, *International communication in Heat and Mass Transfer*, 54, 2013, 16-21.

[11] Cortes, C., Vapnik, V., A Novel Operational Partition between Neural Network Classifiers on Vulnerability to Data Mining Bias, *Journal of Software Engineering and Applications*, 7, 2014, 264-272.

[12] Agrawal, R.K., Muchahary, F., Tripathi, M.M., Ensemble of relevance vector machines and boosted trees for electricity price forecasting, *Applied Energy*, 250, 2019, 540-548.

[13] Meyer, D., Leisch, F., Hornik, K., The support vector machine under test, *Neurocomputing*, 55, 2003, 169-186.

[14] Kong, D., Chen, Y., Li, N., Duan, C., Lu, L., Chen, D., Relevance vector machine for tool wear prediction, *Mechanical Systems, and Signal Processing*, 127, 2019, 573-594.

[15] Tipping, M. E., Sparse Bayesian learning and the relevance vector machine, *Journal of Machine Learning Research*, 1, 2001, 211-244.

[16] Gowthaman, P.S., Jeyakumar, S., A Review on machining of High-Temperature Aeronautics Super-alloys using WEDM, *Materialstoday PROCEEDINGS*, 18, 2019, 4782-4791.

[17] Yan, J., Liu, Y., Han, S., Qiu, M., Windpower grouping forecasts and its uncertainty analysis using optimized relevance vector machine, *Renewable and Sustainable Energy Reviews*, 27, 2013, 613-621.

[18] Feng, Z., Wang, R., Self-validating Pneumatic Actuator Fault Diagnosis Based on Relevance Vector Machine, *International Journal of Control and Automation*, 7, 2014, 181-200.

[19] Tipping, M.E., Bayesian inference: An introduction to principles and practice in machine learning, *Advanced Lectures on Machine Learning*, 3176, 2003, 41-62.

[20] Cheng, Y., Fang, H., A hybrid prognostic method for system degradation based on particle filter and relevance vector machine, *Reliability Engineering & System Safety*, 186, 2019, 51-63.

[21] Ay, M., Stemmler, S., Schwenzer, M., Abel, D., Bergs, T., Model Predictive Control in Milling based on Support Vector Machines, *IFAC-Papers Online*, 52, 2019,1797-1802.

ORCID iD

Hadi Tagimalek https://orcid.org/0000-0001-5451-7564
Mohammad Reza Maraki https://orcid.org/0000-0002-4469-5305
Masoud Mahmoodi https://orcid.org/0000-0002-7446-6140
Majid Azargoman https://orcid.org/0000-0003-2204-7128

Publisher's Note Shahid Chamran University of Ahvaz remains neutral with regard to jurisdictional claims in published maps and institutional affiliations.